

Effects of Neutron Irradiation on Carbon Doped MgB₂ Wire Segments

R. H. T. Wilke, S. L. Bud'ko, P. C. Canfield, and D. K. Finnemore

Ames Laboratory US DOE and Department of Physics and Astronomy, Iowa State University, Ames, IA 50011

Raymond J. Suplinskas[†]

Specialty Materials, Inc., 1449 Middlesex Street, Lowell, Massachusetts 01851

J. Farmer

Missouri University Research Reactor, University of Missouri - Columbia, Research Park, Columbia, MO 65211

S. T. Hannahs

National High Magnetic Field Laboratory, Florida State University, 1800 E. Paul Dirac Drive, Tallahassee, Florida 32310

Abstract

We have studied the evolution of superconducting and normal state properties of neutron irradiated Mg(B_{0.962}C_{0.038})₂ wire segments as a function of post exposure annealing time and temperature. The initial fluence fully suppressed superconductivity and resulted in an anisotropic expansion of the unit cell. Superconductivity was restored by post-exposure annealing. The upper critical field, H_{c2}(T=0), approximately scales with T_c starting with an undamaged T_c near 37 K and H_{c2}(T=0) near 32 T. Up to an annealing temperature of 400 °C the recovery of T_c tends to coincide with a decrease in the normal state resistivity and a systematic recovery of the lattice parameters. Above 400 °C a decrease in order along the c- direction coincides with an increase in resistivity, but no apparent change in the evolution of T_c and H_{c2}. To first order, it appears that carbon doping and neutron damaging effect the superconducting properties of MgB₂ independently.

Key words: MgB₂, carbon doping, neutron irradiation

PACS: 74.25.Bt; 74.25.Fy; 74.25.Ha

1 Introduction

Neutron irradiation and carbon doping of MgB_2 are two methods by which defects can systematically be introduced. Carbon enters the structure replacing boron [1,2] and electron dopes the system, which results in a suppression of T_c [3]. Carbon presumably acts as a point defect, enhancing scattering primarily within the π band [3] which leads to an enhancement of H_{c2} at low doping levels [4] in accordance with theoretical calculations [5]. Up to a doping level of 10%, two gap superconductivity is preserved [6] and evidence suggests that it may persist down to $T_c=0$ [7].

Due to the high neutron capture cross section of ^{10}B , neutron irradiation studies have varied as researchers have employed different techniques to ensure uniform damage throughout samples. The superconducting properties differ depending upon the irradiation conditions. Enhancements in H_{c2} have been observed for neutron irradiation on isotopically enriched Mg^{11}B_2 for fluences of order 10^{17} n/cm² [8], and for irradiation of MgB_2 containing natural boron with a fast neutron fluence of 10^{19} n/cm² [9]. Defects introduced by neutron irradiation, regardless of irradiation conditions, are effective at pinning vortices and for samples which exhibit a T_c above approximately 30 K show enhanced $J_c(H)$ values in the vicinity of 20 K [8,10,11].

We have previously reported on neutron irradiation of MgB_2 filaments [12]. Although the filaments contained natural boron and MgB_2 containing natural boron has a slow neutron half depth of 130 μm , they were 140 μm in diameter and, given that an isotropic neutron flux was used, the damage is believed to be essentially uniform throughout the samples. Irradiating with a fluence level of 4.75×10^{18} n/cm² resulted in a suppression of T_c to below 5 K. Superconductivity was restored by performing post exposure anneals. Upper critical field values were found to approximately scale with T_c . It is believed that the suppression of T_c is a result of both an increase in interband scattering and a decrease in the electron density of states at the Fermi surface. The temperature dependance of the upper critical field exhibits Werthamer, Helfand, and Hohenberg (WHH) [13] like behavior, which suggests the bands become fully mixed, only when T_c is near or below 10 K. The field dependence of the critical current density was found to depend largely upon the superconducting transition temperature. Generally speaking, $J_c(H,T)$ increases for samples with higher T_c values. For example the field at which filaments could carry in excess of 10^4 A/cm² was extended from near 1 T in an undamaged wire to above 1.5 T in the case of a sample whose annealing profile resulted in a T_c near 37 K.

Given that carbon doping appears to weakly decrease T_c and increase H_{c2} by preferentially increasing scattering within the π band, whereas neutron dam-

aging appears to decrease T_c and H_{c2} by increasing the inter-band scattering, the focus of this paper is to examine the effects of combining these two scattering mechanisms by inducing and removing the effects of neutron damage in carbon doped MgB_2 samples. This will allow us to add and subtract inter-band scattering in samples with already enhanced intra- π -band scattering.

2 Experimental Methods

Carbon doped, $Mg(B_{.962}C_{.038})_2$, was prepared in a two step reaction process as described in detail elsewhere [14]. Carbon doped boron filaments, produced by Specialty Materials, Inc., were exposed to excess Mg vapor while the temperature was ramped from 650 °C to 1200 °C over 96 hours. Three filaments, each approximately 5 mm in length, were sealed in quartz ampoules under a He atmosphere and irradiated with an isotropic fluence of 7.13×10^{18} n/cm² reactor neutrons at the Missouri University Research Reactor (MURR), as described in reference [12]. The $Mg(B_{.962}C_{.038})_2$ filaments had a diameter of 110 μ m, indicating the isotropic irradiation should result in essentially uniform damage. The boron filaments used in this study contain a tungsten boride core. Fast neutrons colliding with ¹⁸²W atoms, which have a natural abundance of 26.3%, can be absorbed into the nucleus causing the emission of a proton and transforming the tungsten into ¹⁸²Ta. ¹⁸²Ta β decays back to ¹⁸²W, with a half life of 181 days. As a result the filaments were mildly radioactive and required appropriate safety measures in handling.

Normal state and superconducting properties were determined for a series of post exposure annealing profiles. One set consisted of 24 hour anneals at temperatures up to 600 °C. In the second set the annealing temperature was held constant at 500 °C while the annealing time was varied from 1-1000 hours. In all cases the anneals were performed by placing samples, still sealed with their quartz ampoules, into a Lindberg model 55035 Mini-Mite tube furnace that was preheated to the desired annealing temperature. After the samples were annealed for the desired length of time, the ampoules were removed from the furnace and air quenched to room temperature.

Powder x-ray diffraction (XRD) measurements were made at room temperature using $CuK\alpha$ radiation in a Rigaku Miniflex Diffractometer. Measurements were performed on six filaments from two ampoules. Peak positions were determined by fitting each peak with a Pseudo-Voigt function using Jade analysis software. A silicon standard was used to calibrate each pattern. The experimentally determined Si peak positions were found to be offset from their known values by a constant amount. Within each spectra, the peaks varied about some constant offset and this variation was used to estimate experimental uncertainty in the lattice parameters. Lattice parameters were determined

from the position of the (002) and (110) peaks. DC magnetization measurements and magnetization hysteresis loops were done in a Quantum Design MPMS-5 SQUID magnetometer. For magnetization measurements, individual wires, which have a mass of approximately 0.15 mg, were oriented along the direction of the applied field. Transport measurements were done using a standard four probe AC technique, with platinum wires attached to the samples with Epotek H20E silver epoxy. Typical samples had voltage contacts that were 2-3 mm apart. Resistivity versus temperature in applied fields up to 14 T were carried out in a Quantum Design PPMS-14 system and resistivity versus field was measured up to 32.5 T using a lock-in amplifier technique at the National High Magnetic Field Laboratory in Tallahassee, Florida.

3 Structural Properties

Figure 1 presents the (002) and (110) x-ray peaks for the entire set of 24 hour anneals. In the as-damaged samples both peaks are shifted to lower 2θ , indicating the irradiation resulted in an expansion of the unit cell. The calculated a- and c- lattice parameters yield relative increases with respect to the undamaged sample of $\Delta a=0.0168(7)$ Å and $\Delta c=0.0650(10)$ Å. In the case of neutron irradiation on pure MgB₂, samples exposed to a fluence of 4.75×10^{18} n/cm² showed an increase in the a- and c- lattice parameters of $0.0113(7)$ Å and $0.0538(9)$ Å. At a higher fluence of 9.50×10^{18} n/cm² a greater expansion of the lattice parameters was observed, with a- and c- increasing by $0.0141(9)$ Å and $0.0596(12)$ Å, respectively [12]. Thus the magnitude of the increase in the lattice parameters is greater in the case of the carbon doped MgB₂ samples than was observed in pure MgB₂ samples even when they are exposed to a higher fluence level.

As the annealing temperature is increased up to a temperature of 400 °C we see a systematic shift of both the (002) and (110) peaks to higher 2θ , indicating a contraction of both the a- and c- lattice parameters. At 400 °C the a-lattice parameter appears to reach a minimum, measuring $3.0769(11)$ Å, which is $0.0020(13)$ Å or 0.065% larger than the undamaged sample. The c-lattice parameter decreases monotonically as a function of temperature up to 400 °C, where it has a value of $3.5466(12)$ Å, which is $0.0314(14)$ Å or 0.89% larger than the undamaged value. For anneals at 450 °C and above, a qualitative change in the evolution of the x-ray peaks occurs. The (002) peaks begin to broaden substantially (Figure 2). For the 450 °C and 500 °C anneals, the stable peak refinements for the (002) peak were unattainable, preventing us from attaining estimates of the c- lattice parameter. The corresponding (110) peaks shift to lower 2θ , indicating that the a- lattice parameter may be expanding slightly. After annealing at 600 °C for 24 hours, the (002) peak appears to bifurcate, and indexing as two different peaks yields one Δc value

which is comparable to that attained for an annealing at 400 °C and another which is considerably lower (Figure 3). The (110) peak position, and hence calculated Δa , is comparable to that of the 400 °C anneal. The full set of calculated changes in lattice parameters relative to the undamaged samples for the series of 24 hour anneals is plotted in figure 3. Included in figure 3 is the evolution of the relative change in the lattice parameters as a function of annealing temperature for a pure MgB₂ sample exposed to a fluence of 4.75×10^{18} n/cm² from reference [12].

The (002) and (110) x-ray peaks for a series of samples annealed at 500 °C for times up to 1000 hours are shown in figure 4a. The (002) peaks continue to broaden as the annealing time at 500°C is increased. Stable peak refinements for the (002) peaks were unattainable due to their distorted shape. The (110) peaks monotonically shift to higher 2θ as a function of annealing time up to 96 hours, at which point the a- lattice parameter is within experimental error of the undamaged value (Figure 4b). While the a- lattice parameter is larger for the case of the 24 hour anneal at 500 °C relative to the 24 hour anneal at 400 °C, increasing the annealing time to 96 hours at 500 °C results in a continued contraction of a. Extending the annealing time an additional order of magnitude results in a negligible change in a. It appears that continued annealing at 500 °C causes the structure to become more disordered in the c- direction while the a- lattice parameter is returned to near the undamaged value.

4 Thermodynamic and Transport Measurements

Magnetization and transport measurements were performed to determine the evolution of T_c , H_{c2} , and normal state resistivity as a function of annealing time and temperature. T_c was determined using an onset criteria in resistivity measurements and a 1% screening criteria in magnetization. Figure 5a presents normalized magnetization curves for the entire set of one day annealed samples. As the annealing temperature is increased, the transition temperature monotonically approaches the undamaged value of 36.8 K. It is worth noting that all of the $M(T)$ curves show sharp transitions.

Resistivity versus temperature data is plotted in figure 5b. Normal state resistivity values decrease monotonically as a function of annealing temperature up until $T_{anneal}=450$ °C, at which point ρ_0 increases approximately by a factor of four. The exact cause of this jump in ρ_0 is unknown, but it coincides with the broadening of the (002) x-ray peak. Subsequent increases in the annealing temperature result in decrease in ρ_0 relative to the $T_{anneal}=450$ °C sample. (It has to be mentioned that an alternative way of describing these data is to note that the residual resistivities of samples annealed at 200 °C, 450 °C,

500 °C, and 600 °C are monotonic as a function of the annealing temperature, raising the question as to whether it is the resistivities of the 300 °C and 400 °C annealed samples that are in fact anomalous.) Multiple measurements of samples annealed at 600 °C for 24 hours are included in figure 5b and illustrate the spread in the data. It should be noted that all three of these filaments are from the same quartz ampoule. All three samples show a decrease in resistivity relative to that of the 500 °C annealed sample, but are still above the minimum attained by annealing at 400 °C.

A plot of the normalized, $\rho/\rho(300\text{ K})$, resistivity shows that there are two interesting features in the evolution of the normal state resistivity as a function of annealing temperature (Figure 5c). For the samples annealed at 300 °C and 400 °C, the temperature dependence, $\rho(T)$, has an odd hump in the 100 K to 150 K range. Such a hump was not been observed in pure MgB_2 wires [15] but has been reported for for neutron damaged pure MgB_2 annealed up to a temperature of 400 °C for 24 hours [12]. The trends seen in the calculated normal state resistivity values are also seen in normalized resistivity (Figure 5c), indicating the apparent increase in resistivity occurring at 450 °C is a real effect and not the result of some type of geometrical effect, such as cracking. It should be noted that whereas the transport measurements show changes in the evolution of both ρ_0 and $\rho(T)$ as a function of annealing temperature for samples annealed from 300 °C to 450 °C, the magnetization data showed smooth, sharp transitions with monotonic increases in T_c throughout this range of annealing temperatures.

Magnetization and transport curves for the series of samples annealed at 500 °C for various times are plotted in figure 6. Multiple measurements of samples annealed for 1 hour and 24 hours were performed. The 1 hour anneal transport data consists of sets of two wires from two different ampoules. One set was then used for magnetization measurements and is included along with a filament from a third ampoule. The 24 hour data consists of 2 wires from a single ampoule and an additional filament from a second ampoule. The normalized magnetization transitions for the 1 hour anneals all fall below those of the 24 hour anneals (Figure 6a). However, for the transport data, the range of T_c values is broader and several of the transitions occur at temperatures greater than is seen for the 24 hour anneals (Figure 6b). It should be noted that for the samples annealed at 500 °C for 1 hour for which both magnetization and transport measurements were performed, in both cases the transport data showed a T_c that were approximately 0.5 K to 1 K higher than was observed in the magnetization measurements. Such a spread was also observed in the case of neutron irradiation on pure MgB_2 [12], suggesting the spread in the data is a reflection of sample to sample variation.

The multiple transport measurements on samples annealed at 500 °C for one hour also exhibit considerable spread in the the normal state resistivity values,

and no systematic evolution of ρ_0 as a function of annealing time is observed. Residual resistivity ratios of these samples indicate that the observed spread in resistivity values represents true sample to sample variation in ρ_0 and is not the result of pathologic geometric problems such as cracks.

In the case of samples annealed at 500 °C for various times, generally speaking, extending the annealing time tends to decrease ΔT_c , although there is considerable spread in the data (Figure 7). For neutron irradiated pure MgB₂ wires, ΔT_c , which was taken as a measure of the defect concentration, was found to decrease exponentially with time [12], indicating defects are being annealed out by a single activated process with random diffusion [16]. For such samples, the defect concentration, n , obeys the relation

$$n = n_o e^{\lambda t} \quad (1)$$

where n_o is the initial defect concentration, λ is a rate constant, and t is the time. λ is a function of the activation energy, E_a , and diffusion coefficients. For samples which do show an exponential behavior in the decrease of ΔT_c (and by presumption) the defect density as a function of annealing time the activation energy can be determined by the so-called cross-cut procedure [16]. This involves comparing the annealing time for which different temperature anneals reached the same defect density, i.e. ΔT_c . If a ΔT_c is reached by annealing at a temperature T_1 for a time t_1 and by annealing at a temperature T_2 for a time t_2 , then the activation energy is related to these quantities by:

$$\ln \frac{t_1}{t_2} = \frac{E}{k} \left(\frac{1}{T_1} - \frac{1}{T_2} \right). \quad (2)$$

Unfortunately, we did not have a sufficient number of samples to perform studies of the temperature dependance of ΔT_c as a function of annealing time at any temperatures other than 500 °C. However, if we assume that the primary difference between neutron irradiation of pure and carbon doped MgB₂ is in the activation energies, then we can gain some insight by comparing λ values attained from the two sets of samples. For the case of the carbon doped samples, since the spread in T_c for a given annealing time is so large, we can obtain only a rough estimate, based on a fitting of the midpoint of the T_c values. Such a calculation yields a rate constant of $\lambda=1.61 \text{ s}^{-1}$. For irradiation on pure MgB₂ anneals at 200 °C, 300 °C, and 400 °C yielded rate constants of 2.77 s^{-1} , 2.21 s^{-1} , and 3.51 s^{-1} respectively [12]. Although there is considerable spread in the rate constants for the pure MgB₂ case, and considerable uncertainty in the rate constant associated with the carbon doped MgB₂ samples (estimates of λ from raw data range from 1.00 s^{-1} to 2.03 s^{-1}) analysis of equation 2 shows that since carbon doped samples have a lower rate constant than pure MgB₂ samples the activation energy is higher for carbon

doped samples. It should be noted that higher reaction temperatures were required to synthesize carbon doped MgB₂ than pure MgB₂ [14], suggesting that there are different energy scales associated with carbon doping.

Upper critical field values were determined using the onset criteria in both resistivity versus temperature in applied fields up to 14 T and resistivity versus field in field sweeps up to 32.5 T (Figure 8). The complete H_{c2}(T) curves for the entire set of annealing profiles is given in figure 9. The set forms a sort of "Russian doll pattern," with H_{c2}(T=0) approximately scaling with T_c. Such behavior was also observed for neutron irradiation and post-exposure anneals on pure MgB₂ filaments [12].

Critical currents densities were estimated from magnetization hysteresis loops using the Bean Critical State Model [17] for cylindrical geometry. Figure 10a shows the field dependence of J_c at T=5 K for the entire set of 24 hour anneals at various annealing temperatures. For the set of one day anneals, the in field performance improves with annealing temperature, up to 500 °C. Presumably the increase transition temperature and hence decreased reduced temperature (T/T_c) of the measurement, is the primary cause of the enhancement. However, there exists a much greater increase in in-field J_c values between the sample annealed at 400 °C and the sample annealed at 450 °C than between the sample annealed at 300 °C and the sample annealed at 400 °C. Whereas increasing the annealing temperature from 300 °C to 400 °C results in a near 7 K or 36% increase in T_c but only a factor of two improvement in J_c at all fields, increasing the annealing temperature from 400 °C to 450 °C results in only an additional 5 K increase or 17% increase in T_c, but nearly an order of magnitude increase in in-field J_c values. This suggests the increase in disorder between the hexagonal planes, which coincided with an increase in resistivity, may also play a role in enhancing the flux pinning. The sample annealed at 600 °C shows slightly reduced J_c(H) values relative to the 500 °C anneal. Thus, at 600 °C, either the increased order along c is diminishing J_c, or we are beginning to anneal out some of the defects which are effective at pinning vortices, or some combination thereof.

Extending the annealing time from 1 hour to 96 hours at 500 °C results in relatively minor increases in in-field J_c values (Figure 10b). The data for the 500 °C and 96 hour anneal is particularly noisy and may not truly be enhanced relative to the 500 °C/10³ hour anneal. All of these 500 °C anneals show J_c remaining fairly constant over the field range of 1-4 Tesla.

At 5 K, the best in field performance, which results from the 96 and 1000 hour anneals at 500 °C, yield J_c values which maintain 10⁴ A/cm² in an applied field of 4 T. In comparison, the best in field performance at 5 K for a sample of neutron irradiated pure MgB₂ dropped below 10⁴ A/cm² in an applied field of approximately 1.5 T [12] and an undamaged carbon doped filament dropped

below this level near 1 T [14].

5 Discussion

Up to an annealing temperature of 400 °C, the behavior of irradiated carbon doped samples is quite similar to that of irradiation of pure MgB₂ filaments. As-damaged samples have expanded unit cells and suppressed superconducting transition temperatures. Post exposure annealing tends to return the lattice parameters and T_c towards the undamaged values. In both cases, the upper critical field values, $H_{c2}(T=0)$ tend to scale with T_c .

The intriguing aspect of neutron damage in the carbon doped samples is the temperature induced decrease in structural order in the c- direction which occurs near $T_{anneal}=450$ °C. No such effect was seen in the case of neutron irradiation in pure MgB₂ filaments. The feature doesn't appear to be a phase segregation as no double transition is seen in magnetization. Furthermore, samples annealed at 500 °C showed sharp, single transitions in both magnetization and resistivity, while the having broad (002) peaks. The sample annealed for 24 hours at 600 °C showed evidence of having two distinct phases with different c- lattice parameters but the same a- lattice parameter. Here again, both the magnetization and transport data showed only single transitions. Thus the transition temperature appears to be insensitive to the c- lattice parameter. The a- lattice parameter is presumably not the sole determining factor for T_c , as samples annealed for 24 hours at 450 °C and 500 °C showed increases in Δa relative to the sample annealed for 24 hours 400 °C, while also having increased T_c values. It should be noted that although measurements on single filaments showed sharp, single transitions, there was significant spread in the T_c values between different samples.

The broadening of the (002) peak coincides with a near 4 fold increase in the normal state resistivity and approximate order of magnitude increase in in-field J_c values. Increases in normal state resistivity for annealing temperatures above 400 °C have been observed in neutron irradiation of pure MgB₂ [18]. In this case, the authors report a continued increase in ρ_0 as a function of annealing temperature above 400 °C and attribute it to a loss of intergrain connectivity. In contrast our data show a decrease in ρ_0 for 24 hour anneals at 500 °C and 600 °C, which supports the notion that a different mechanism is responsible for the anomalous behavior in the normal state resistivity of neutron irradiated carbon doped samples.

Despite the decrease in structural order along the c- axis and large increase in resistivity at $T_{anneal}=450$ °C, no qualitative changes to the evolution of T_c and H_{c2} as a function of annealing temperature were observed. The transi-

tion temperature tends to approach that of the undamaged sample and H_{c2} continues to roughly scale with T_c . Even the 500 °C, 1000 hour anneal shows a suppressed $H_{c2}(T=0)$ value relative to the undamaged sample. This is in contrast to the results obtained with irradiation of pure MgB_2 filaments [12]. For fluence levels of 4.75×10^{18} n/cm² and 9.50×10^{18} n/cm², two values which envelop the 7.13×10^{18} n/cm² fluence level used in this study, $H_{c2}(T=0)$ was enhanced by approximately 2 T and 3 T respectively.

Both pure and carbon doped samples show increases in normal state resistivity after annealing (Figure 11). Pure MgB_2 wires irradiated with a fluence of 4.75×10^{18} n/cm² and subsequently annealed for 24 hours at various temperatures showed an increase in ρ_0 at an annealing temperature of 200 °C. In contrast, for $Mg(B_{.962}C_{.038})_2$ filaments exposed to a fluence of 7.13×10^{18} n/cm² and subsequently annealed for 24 hours at various temperatures, the apparent anomalous increase occurs for an annealing temperature of 450 °C. For both sets of samples, following the abrupt increase, the normal state resistivity decreases monotonically as a function of annealing temperature. It should be noted however, that, in the case of the carbon doped samples, it is not clear whether or not there exists some correlation between the change in the temperature dependence of the normal state resistivity for the 300 °C and 400 °C anneals and the reduced ρ_0 values for these anneals. That is, rather than the jump in ρ_0 at 450 °C representing an anomalous increase, the ρ_0 values associated with the samples annealed at 300 °C and 400 °C may in fact be anomalously low.

These data, coupled with the analysis of the rate constants, suggest that in the case of neutron irradiated carbon doped MgB_2 samples, there is a different, and higher, energy scale associated with the annealing of defects. This is perhaps not altogether surprising, as it was shown that higher reaction temperatures were necessary to form the carbon doped phase. Whereas pure boron filaments can be fully converted to MgB_2 in as little as 2 hours at 950 °C [19], isothermal reactions required 48 hours at 1200 °C to convert carbon doped boron fibers to $Mg(B_{1-x}C_x)_2$, even for doping levels as low as $x=0.004$ [14]. Although diffusion of Mg vapor into a carbon doped boron matrix and repair of neutron induced damage are indeed two, rather different, phenomena, this correlation is at least worth noting.

The temperature dependence of the upper critical field shows positive curvature near T_c for samples with a T_c near 26 K and above (Figure 9). For the samples annealed for 24 hours at 200 °C and 300 °C H_{c2} approaches T_c linearly. If the two bands are fully mixed, the temperature dependence of the upper critical field should follow WHH [13] behavior, where $H_{c2}(T=0)$ is given by:

$$H_{c2}(T = 0) = 0.69T_c \frac{dH_{c2}}{dT}. \quad (3)$$

Calculating $H_{c2}(T=0)$ using equation 3 for the samples annealed for 24 hours at 200 °C, 300 °C, and 400 °C yields values of 2.4 T, 5.2 T, and 6.5 T. Experimentally, lowest temperate H_{c2} values we could reliably attain from transport measurements for each of these samples were 2.1 T, 6.5 T, and 10 T, occurring at temperatures of 4.2 K, 5.2 K, and 4.6 K respectively. Only for the sample annealed at 200 °C does the WHH fit yield an $H_{c2}(T=0)$ value which is consistent with the experimentally observed data. Thus it is likely that only for samples with a T_c below 10 K are the bands fully mixed. Such a result was also obtained in the case of the neutron irradiation on pure MgB_2 [12]. This implies that the inter-band scattering rates resulting from defects associated with the neutron irradiation are comparable in both pure and carbon doped samples, suggesting that the scattering associated with the two different sources of defects act independently. This is not altogether surprising as the suppression in T_c for carbon doped samples is believed to result from changes in the Fermi surface, rather than increases in inter-band scattering and scattering associated with carbon doping is believed to be primarily within the π band [3]. Thus if inter-band scattering is introduced primarily through defects resulting from neutron damage, if pure and carbon doped samples have similar initial T_c values, then they should also exhibit fully mixed bands at similar T_c s, which was experimentally observed. A similar result was found in the case of neutron irradiation on pure MgB_2 filaments, implying that the scattering associated with carbon doping and neutron irradiation act independently.

6 Conclusions

We have studied superconducting and normal state properties of neutron irradiated carbon doped MgB_2 filaments as a function of post exposure annealing time and temperature. In spite of anomolous behavior in the evolution of the c-lattice parameter and normal state resistivity T_c tended to return towards the undamaged value with increased annealing time and temperature. Upper critical field values were found to approximately scale with T_c and exhibited WHH like behavior, suggesting a complete mixing of the two bands, for samples with T_c near 10 K. Neutron irradiation of pure MgB_2 also led to a complete mixing of the bands near 10 K, suggesting that the scattering associated with carbon doping and neutron irradiation act independently.

Acknowledgements

Ames Laboratory is operated for the U.S. Department of Energy by Iowa State University under Contract No. W-7405-Eng-82. This work was supported by the Director for Energy Research, Office of Basic Energy Sciences. A portion of this work was performed at the National High Magnetic Field Laboratory, which is supported by NSF Cooperative Agreement No. DMR-0084173 and

by the State of Florida.

[†]In the course of this work Raymond J. Suplinskas succumbed to a long term illness. Ray's enthusiastic support and collaboration was vital to much of the success of our MgB₂ research. We will miss him greatly.

References

- [1] R.A. Ribeiro, S.L. Bud'ko, C. Petrovic, and P.C. Canfield, *Physica C* 384 (2003) 227.
- [2] M. Avdeev, J.D. Jorgensen, R.A. Ribeiro, S.L. Bud'ko, P.C. Canfield, *Physica C* 387 (2003) 301.
- [3] M. Angst, S.L. Bud'ko, R.H.T. Wilke, and P.C. Canfield, *Phys. Rev. B* 71 (2005) 144512.
- [4] R.H.T. Wilke, S.L. Bud'ko, P.C. Canfield, D.K. Finnemore, Raymond J. Suplinskas, and S.T. Hannahs, *Phys. Rev. Lett.* 91 (2004) 217003.
- [5] A. Gurevich, *Phys. Rev. B* 67 (2003) 184515.
- [6] P. Samuely, Z. Hořanová, P. Szabó, J. Kačmarčík, R.A. Ribeiro, S.L. Bud'ko, and P.C. Canfield, *Phys. Rev. B* 68 (2003) 020505.
- [7] Z. Hořanová, P. Szabó, P. Samuely, R.H.T. Wilke, S.L. Bud'ko, and P.C. Canfield, *Phys. Rev. B* 70 (2004) 064520.
- [8] M. Putti, V. Braccini, C. Ferdeghini, F. Gatti, P. Manfrinetti, D. Marre, A. Palenzona, I. Pallecchi, C. Tarantini, I. Sheikin, H.U. Aebersold, and E. Lehmann, *App. Phys. Lett.* 86 (2005) 112503.
- [9] Y. Wang, F. Bouquet, I. Sheikin, P. Toulemonde, B. Revaz, M. Eisterer, H.W. Weber, J. Hinderer, and A. Junod, *J. Phys.: Condens. Matter* 15 (2003) 883-893.
- [10] U.P. Trociewitz, P.V.P.S.S. Sastry, A. Wyda, K. Crockett, and J. Schwartz, *IEEE Transactions on Applied Superconductivity* 13 (2003) 3320-3323.
- [11] M. Eisterer, M. Zehetmayer, S. Tönies, H. W. Weber, M. Kambara, N. Hari Babu, D.A. Cardwell, and L.R. Greenwood, *Superconductor Science and Technology* 15 (2002) L9-L12.
- [12] R.H.T. Wilke, S.L. Bud'ko, P.C. Canfield, J. Farmer, and S.T. Hannahs, *cond-mat/0507185*
- [13] N.R. Werthamer, E. Helfand, and P.C. Hohenberg, *Phys. Rev.* 147 (1966) 295.
- [14] R.H.T. Wilke, S.L. Bud'ko, P.C. Canfield, D.K. Finnemore, R.J. Suplinskas, and S.T. Hannahs, *Physica C* 424 (2005) 1.

- [15] P.C. Canfield, D.K. Finnemore, S.L. Bud'ko, J.E. Ostenson, G. Lapertot, C.E. Cunningham, and C. Petrovic, *Phys. Rev. Lett.* 86 (2001) 2423.
- [16] A.C. Damask and G.J. Dienes, *Point Defects in Metals*, Gordon and Breach, Science Publishers, Inc., New York, 1963.
- [17] C.P. Bean, *Phys. Rev. Lett* 8 (1962) 250.
- [18] A.E. Karkin, V.I. Voronin, T.V. Dyachkova, A.P. Tyutyunnik, V.G. Zubkov, Yu. G. Zainulin, and B.N. Goshchitskii, *JETP Letters* 73 (2001) 570.
- [19] C.E. Cunningham, C. Petrovic, G. Laperot, S.L. Bud'ko, F. Laabs, W. Straszheim, D.K. Finnemore, and P.C. Canfield, *Physica C* 353 (2001) 5.

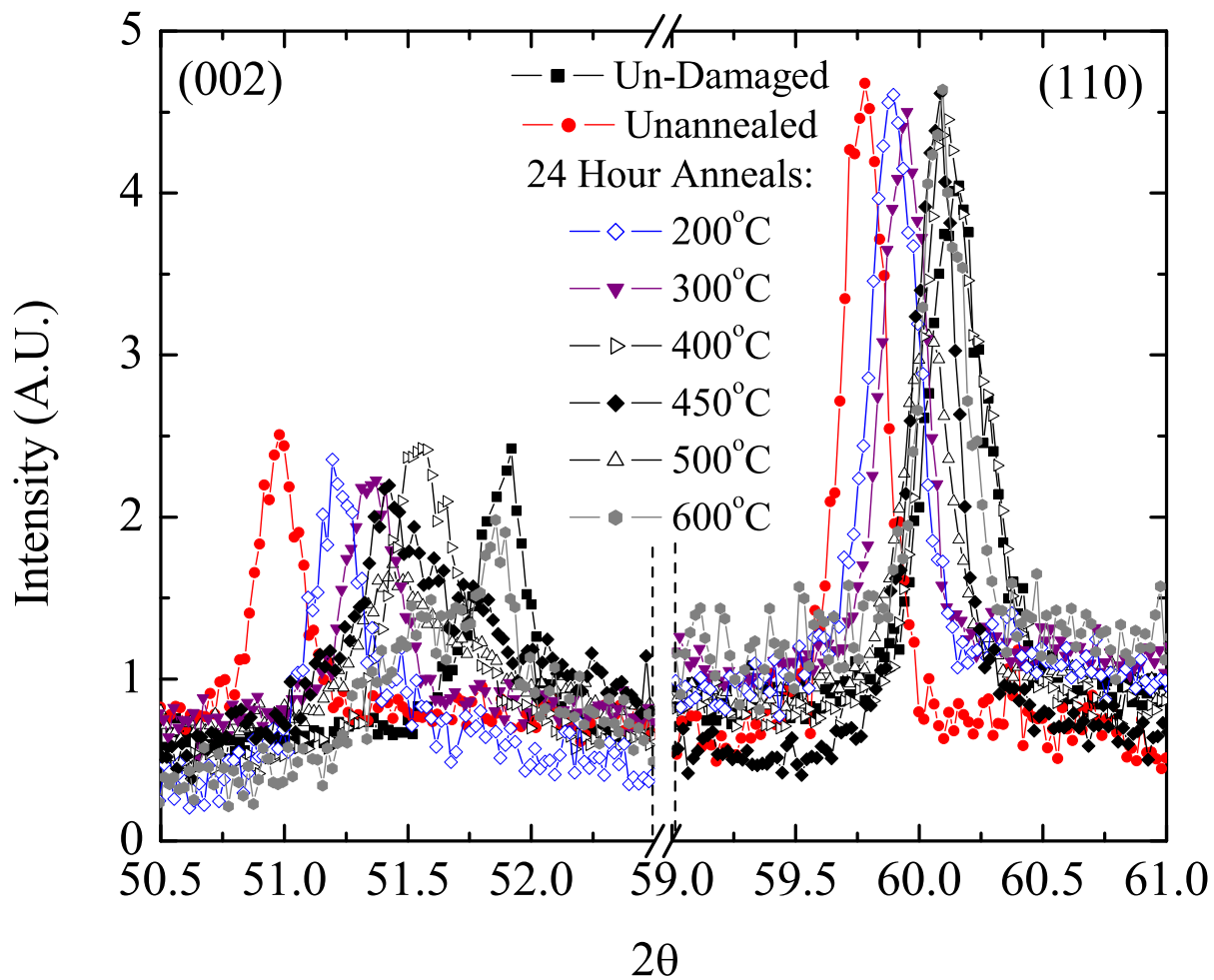


Fig. 1. (002) and (110) x-ray peaks for the series of neutron irradiated $\text{Mg}(\text{B}_{0.962}\text{C}_{0.038})_2$ samples annealed for 24 hours at various temperatures.

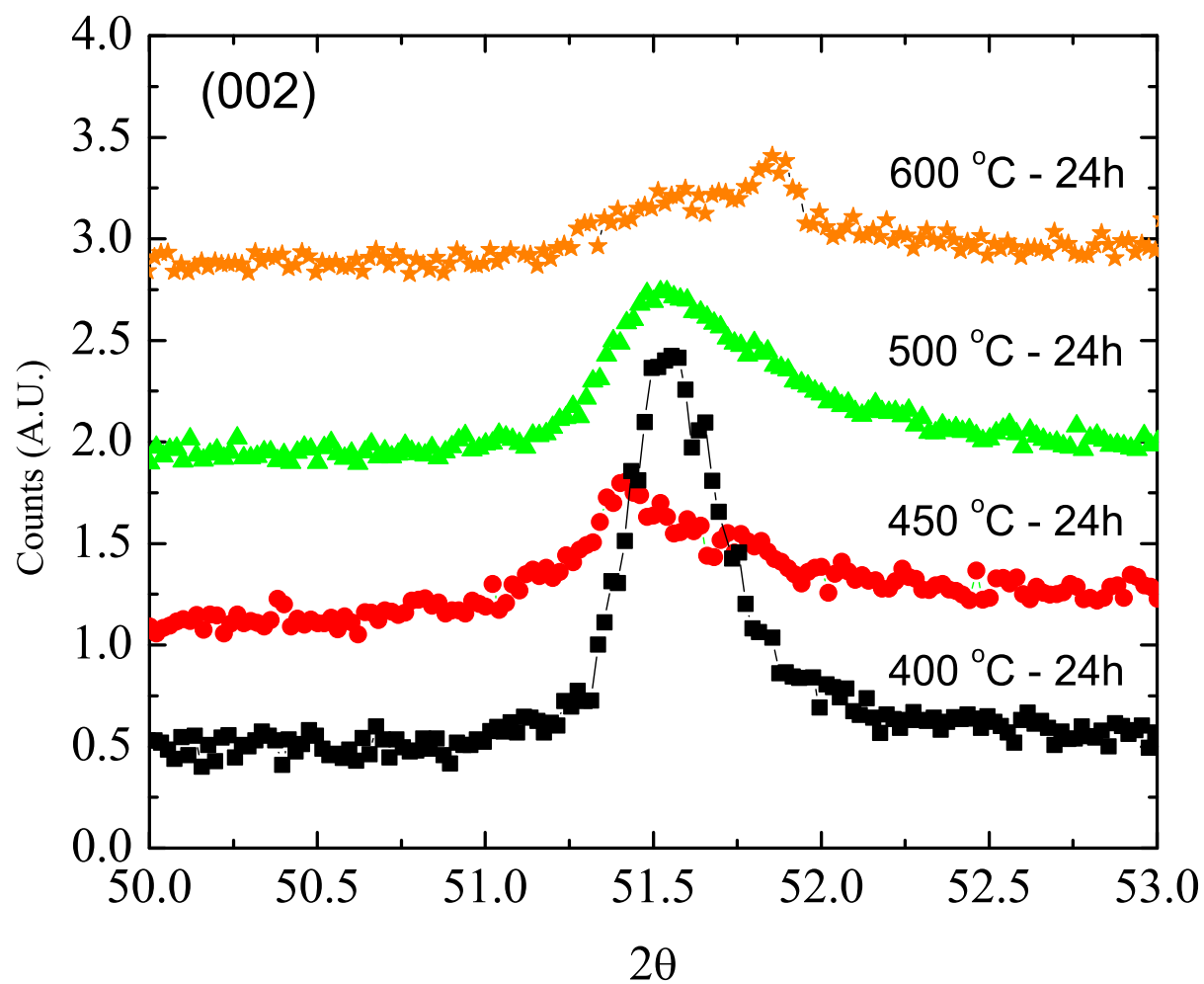


Fig. 2. Evolution of the x-ray (002) peak as a function of annealing temperature for 24 hour anneals.

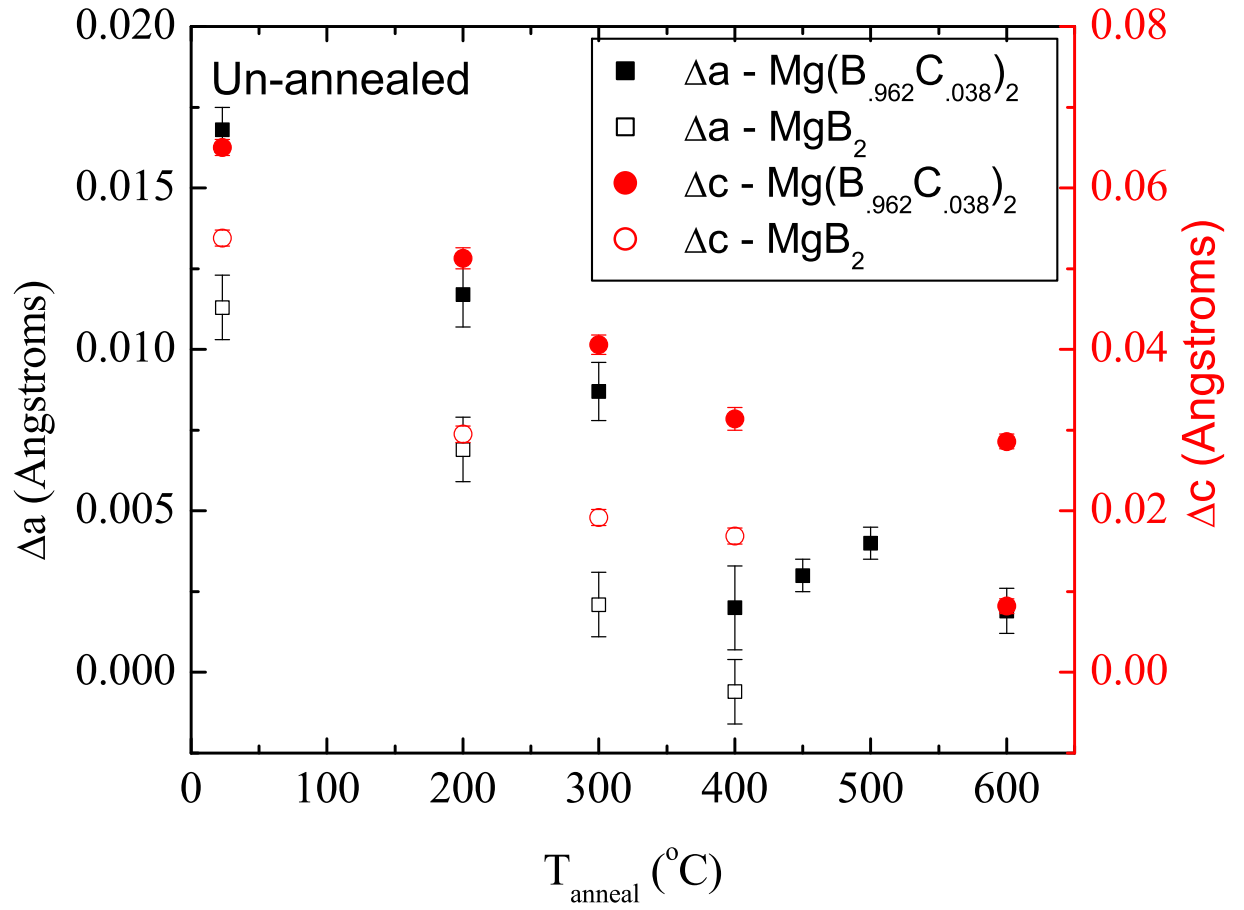
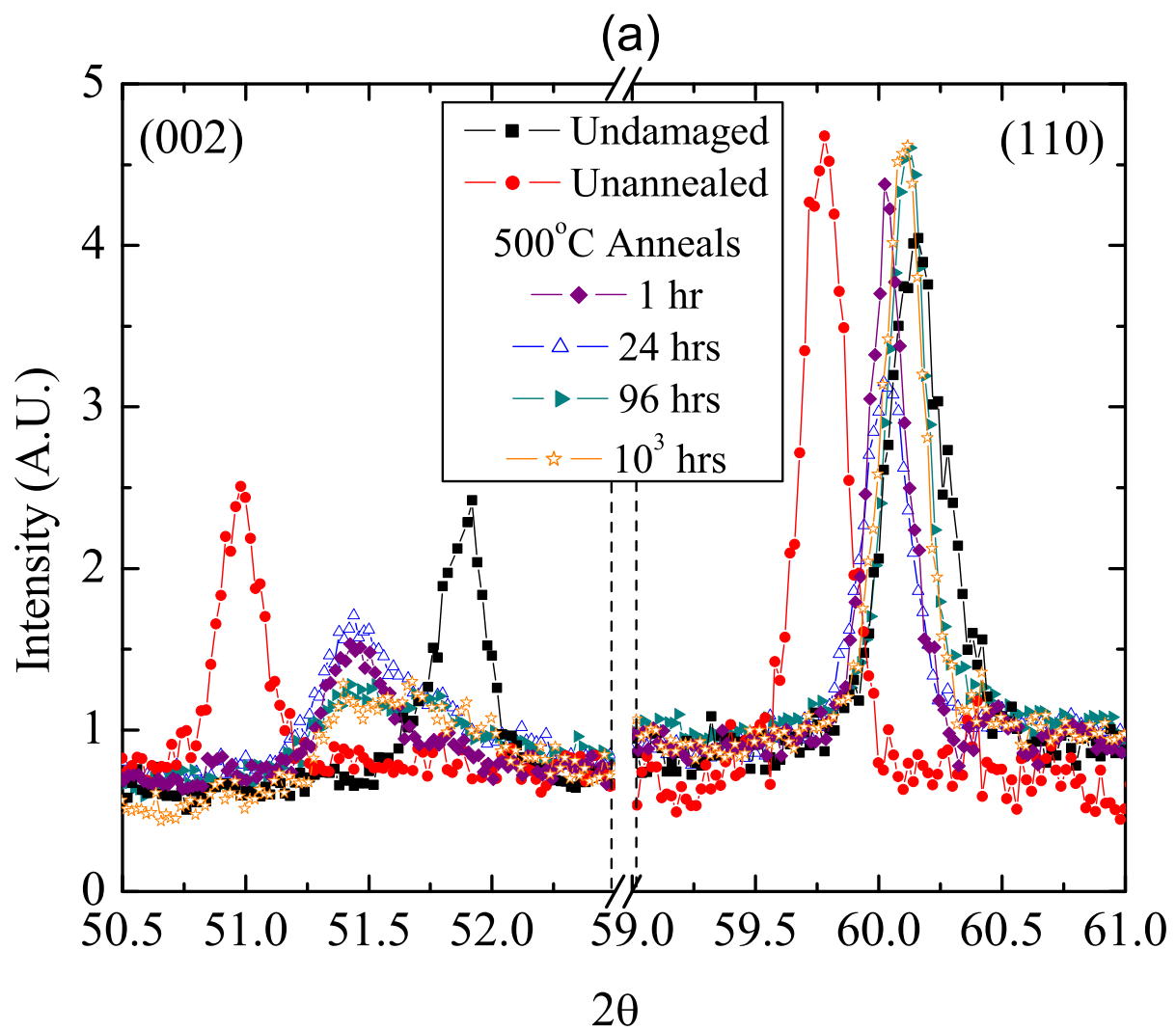


Fig. 3. Lattice parameters as a function of annealing temperature for 24 hour anneals, as calculated from the positions of the (002) and (110) x-ray peaks. Included are data on a pure MgB₂ sample exposed to a fluence of 4.75×10^{18} n/cm² from reference [12].



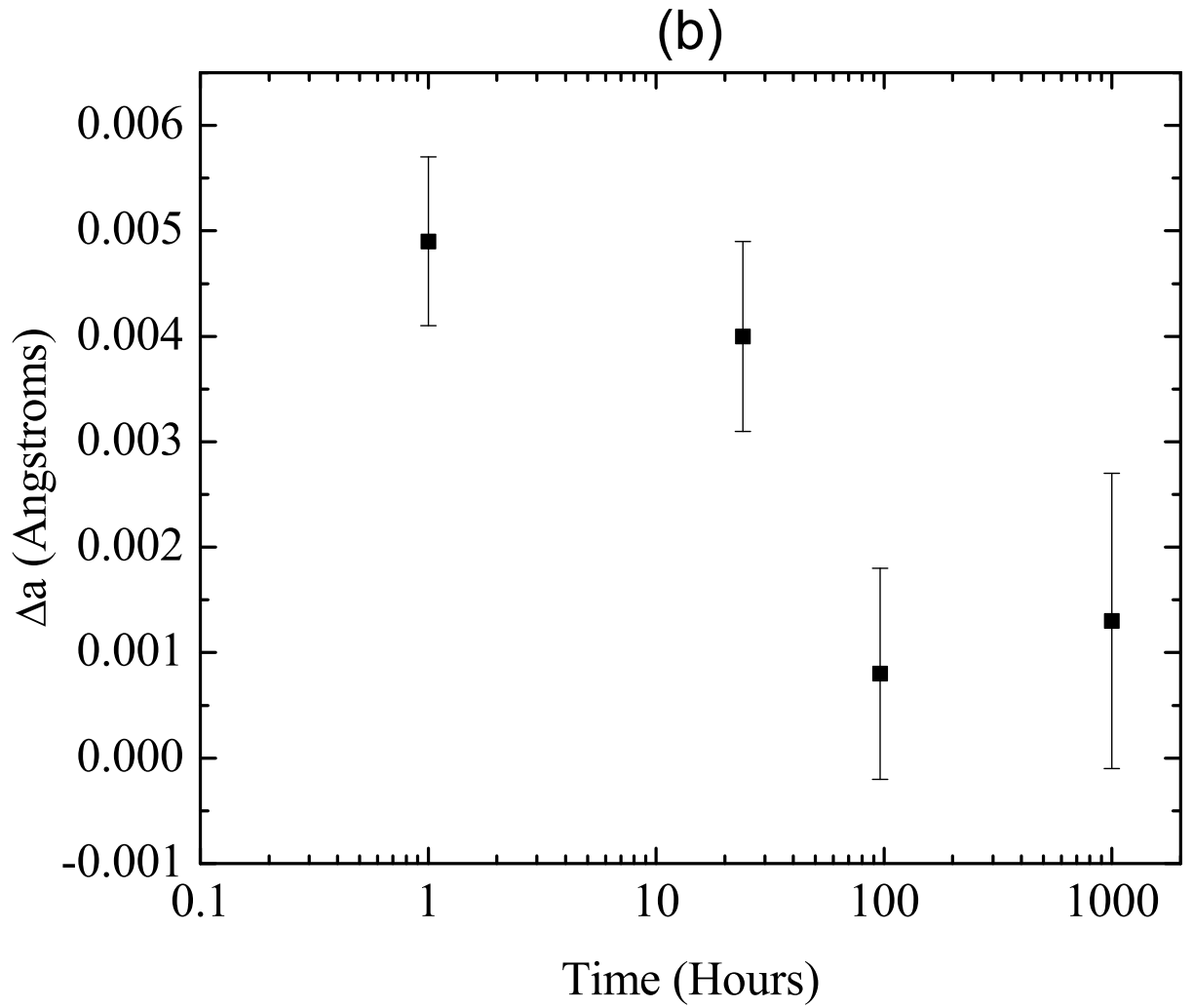
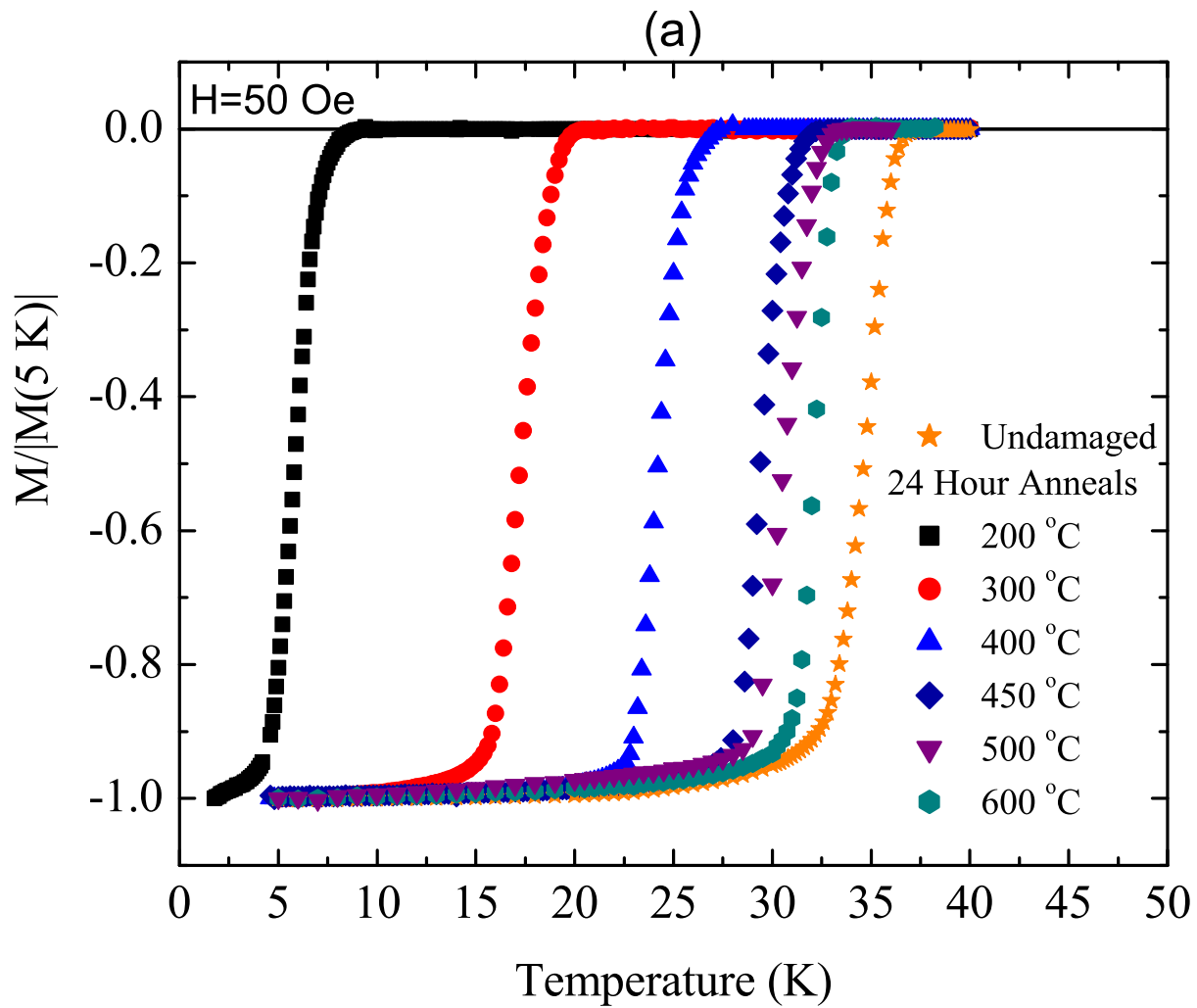
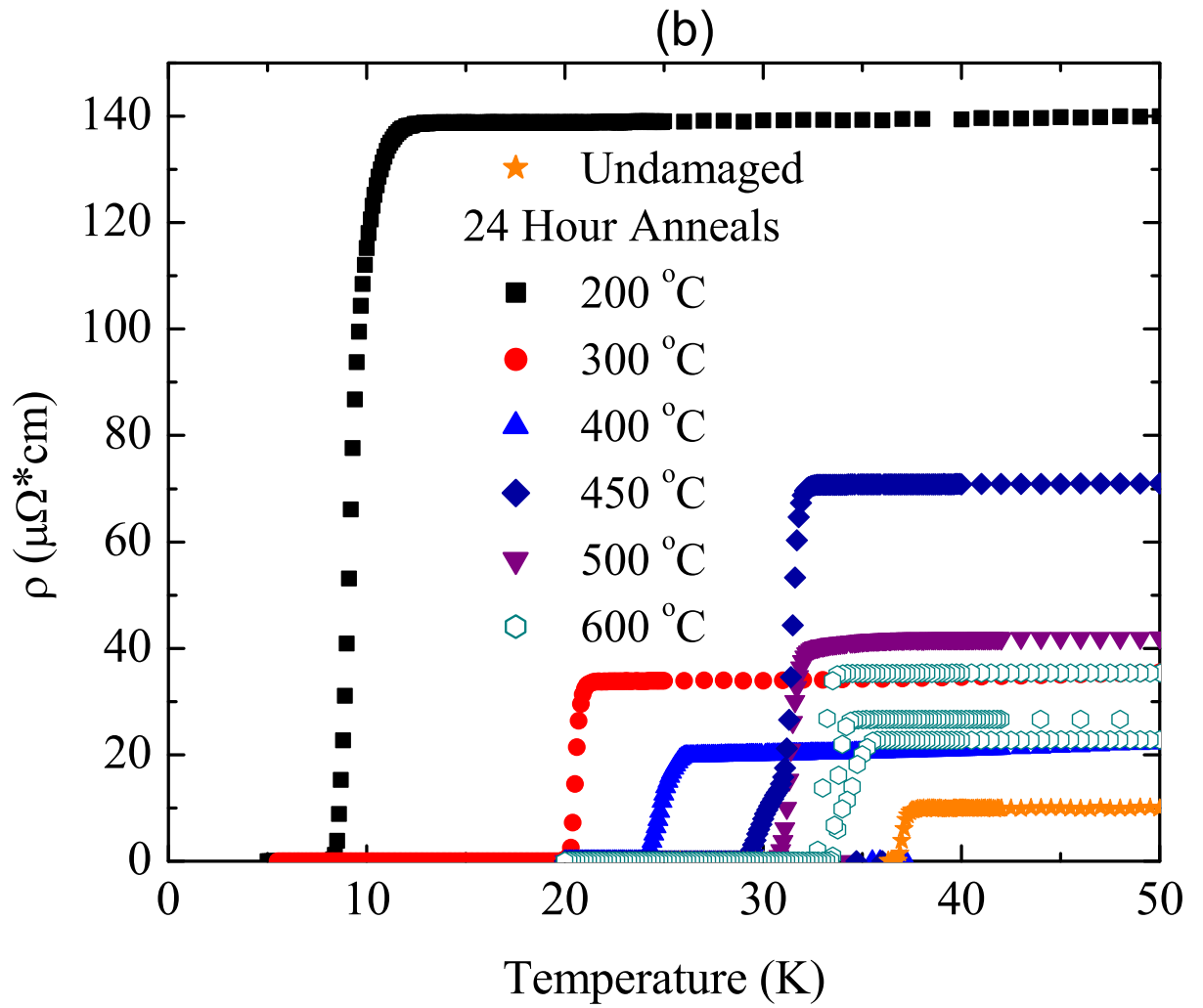


Fig. 4. (a) Evolution of the (002) and (110) x-ray peaks as a function of annealing time at 500 °C. (b) Calculated shift of the a- lattice parameter from the undamaged sample.





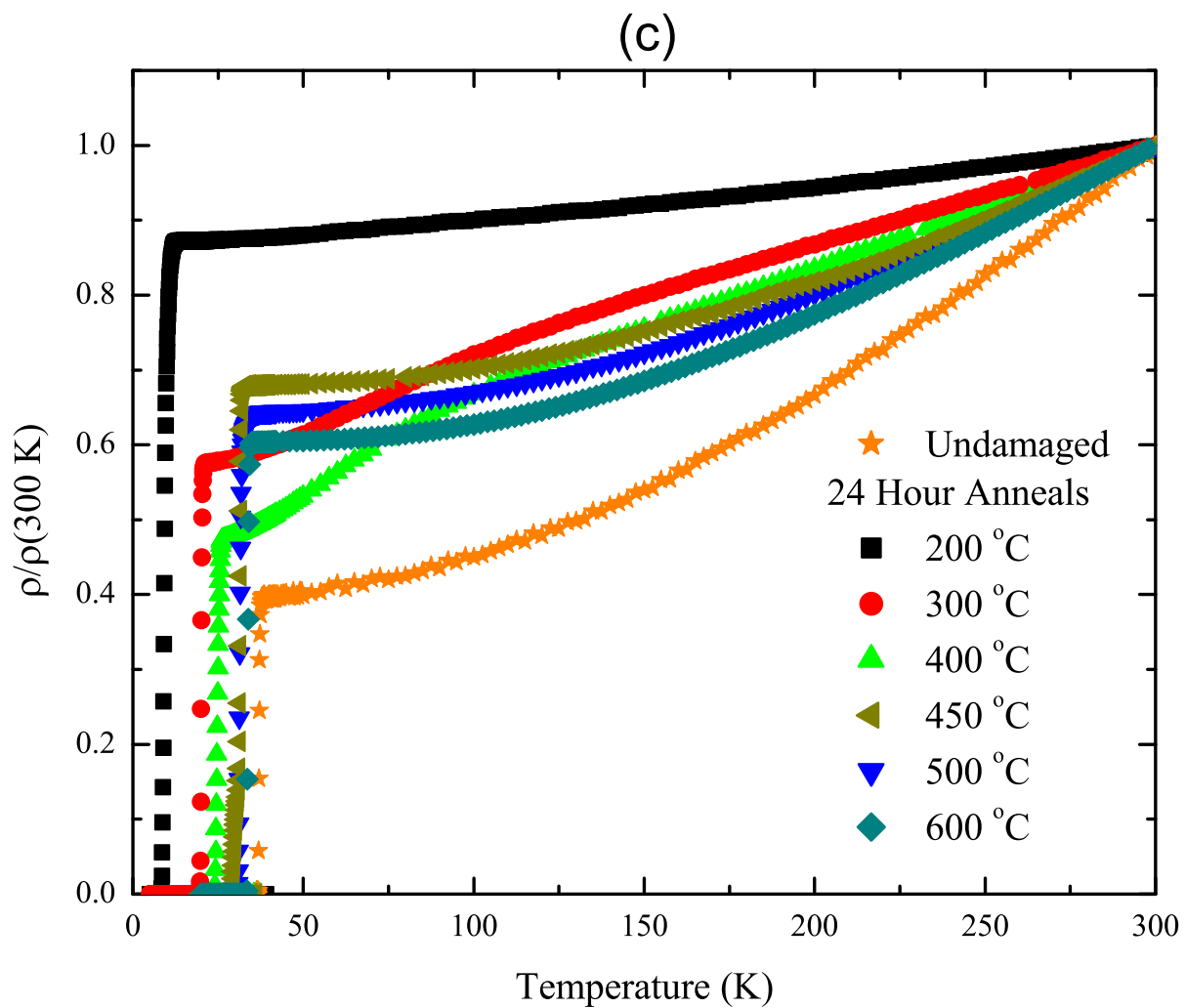
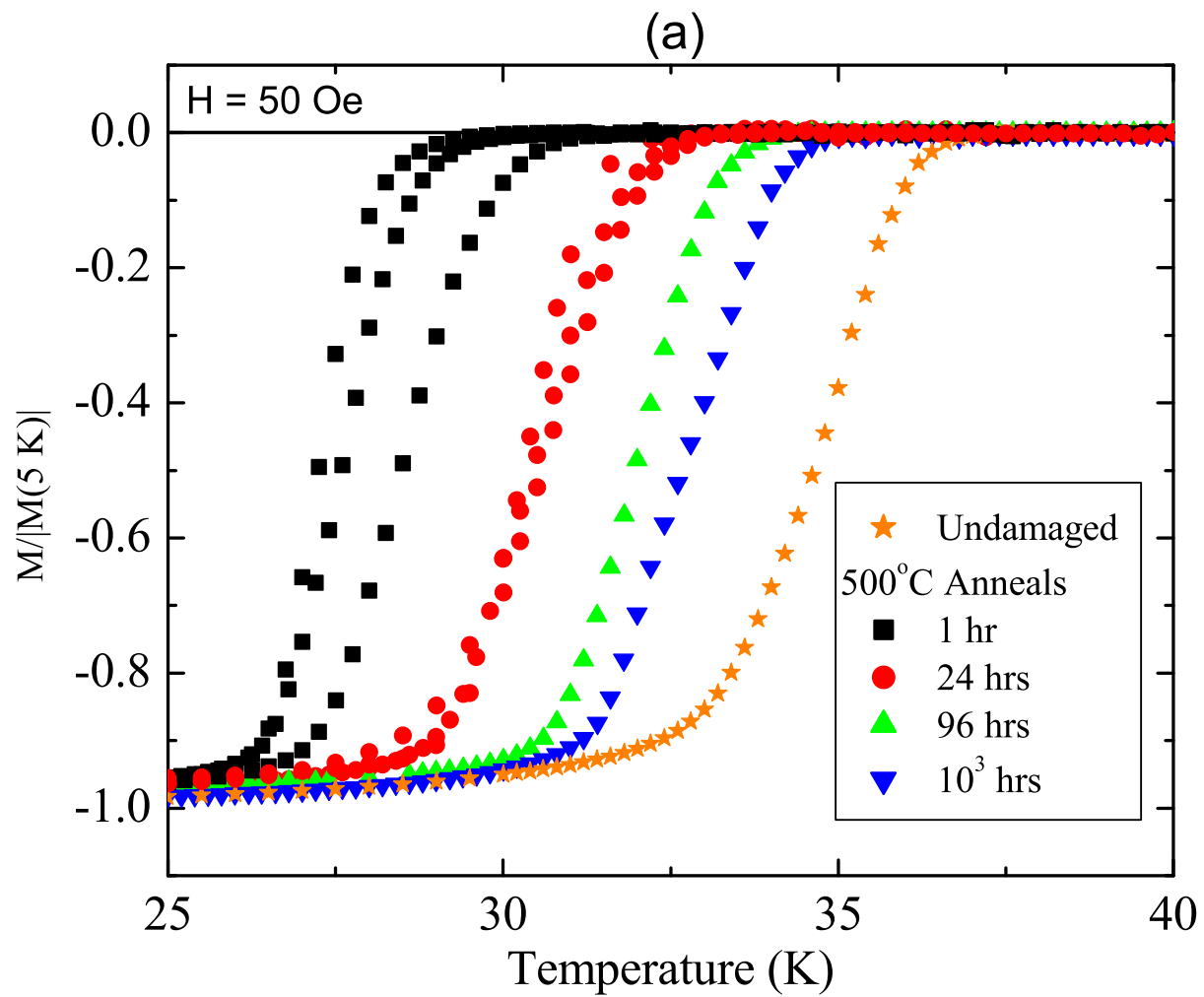


Fig. 5. Normalized magnetization (a) and zero field resistivity curves (b) for samples annealed at various temperatures for 24 hours. (c) Normalized resistivity curves for neutron irradiated $\text{Mg}(\text{B}_{.962}\text{C}_{.038})_2$ samples annealed for 24 hour at various temperatures.



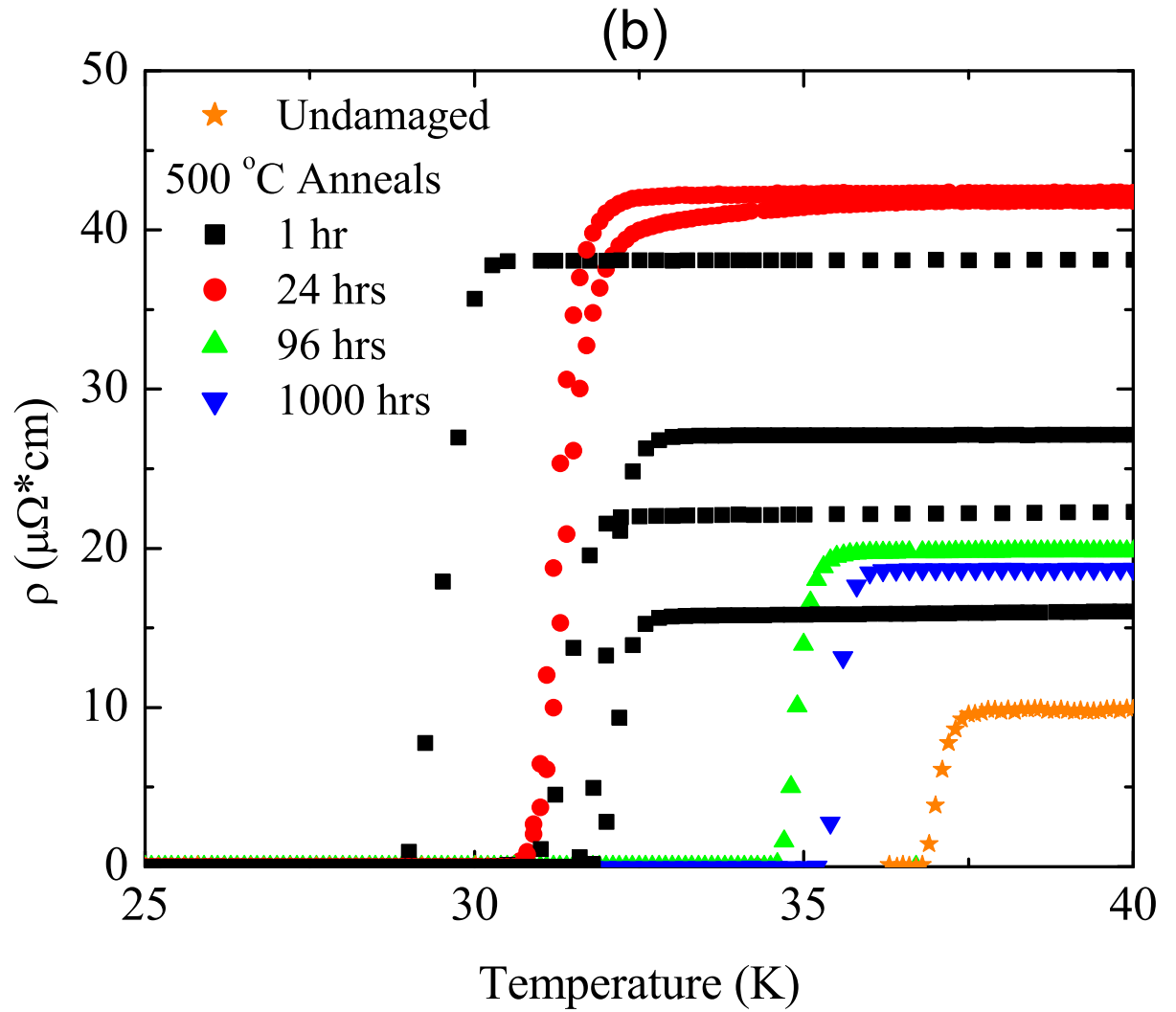


Fig. 6. Normalized magnetization (a) and zero field resistivity curves (b) for samples annealed at various times at 500 °C.

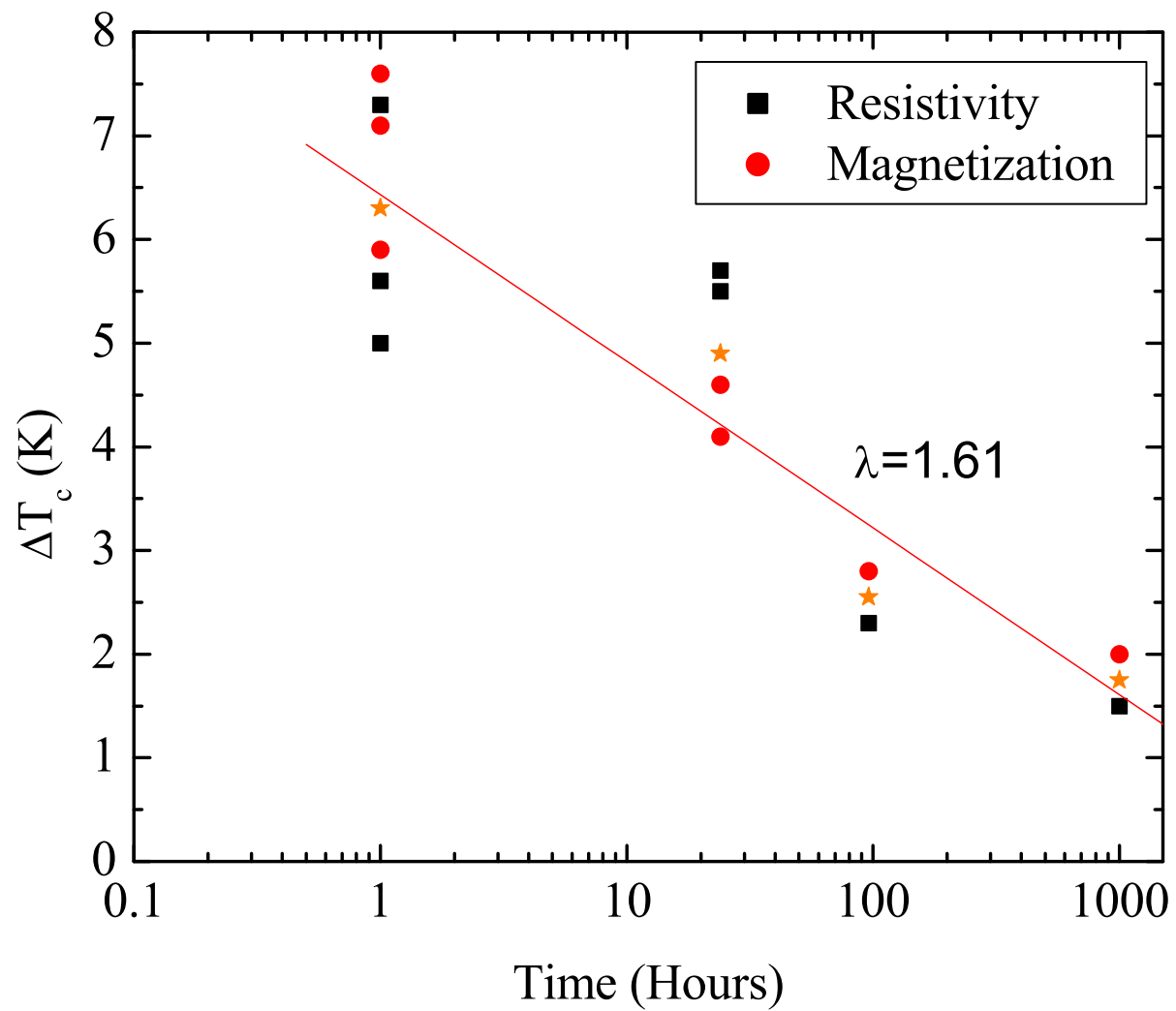
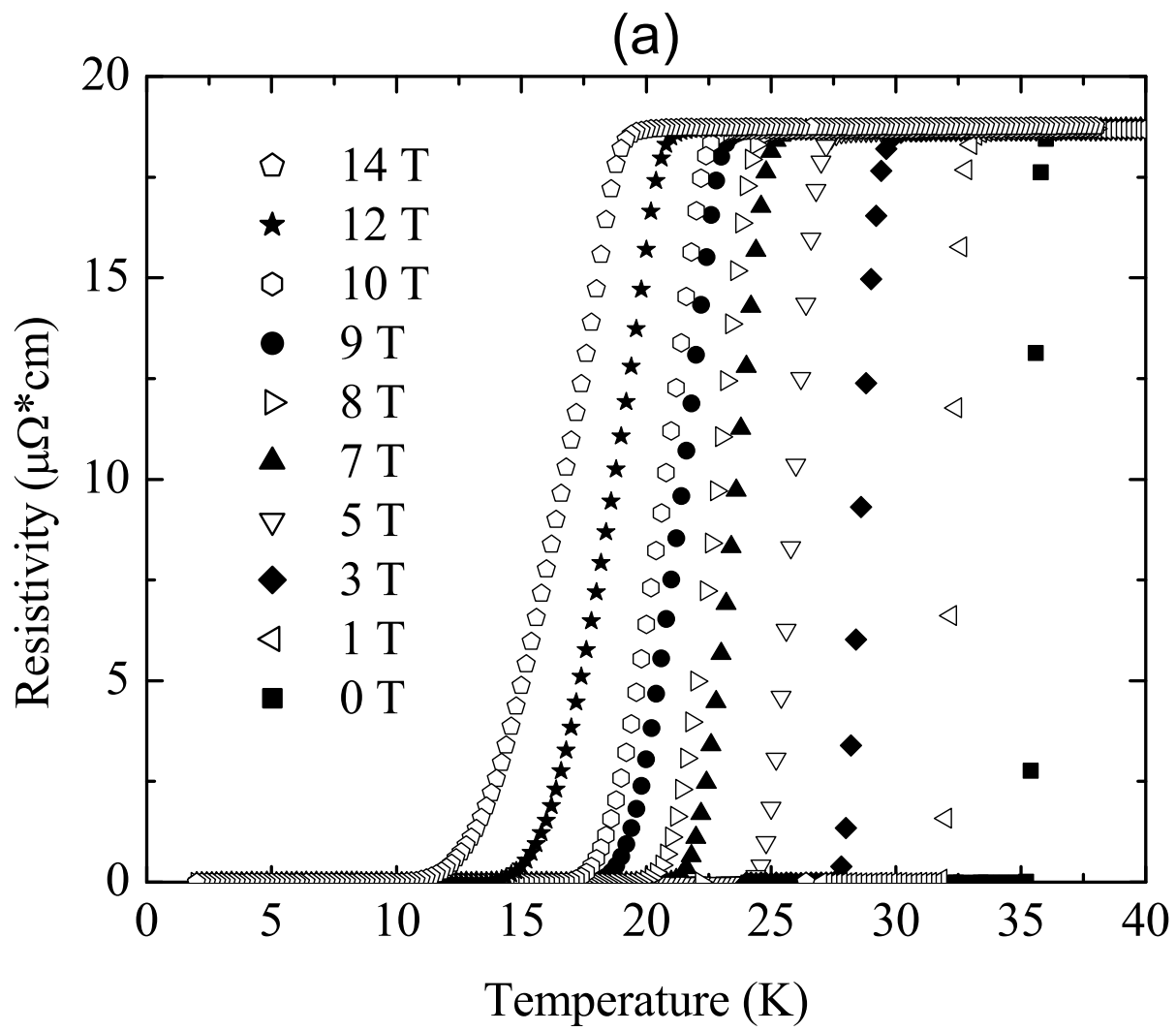


Fig. 7. ΔT_c as a function of time for 500 °C anneals. The stars represent the midpoint of spread for a given time and the rate constant, λ , is determined by a linear fit of these data.



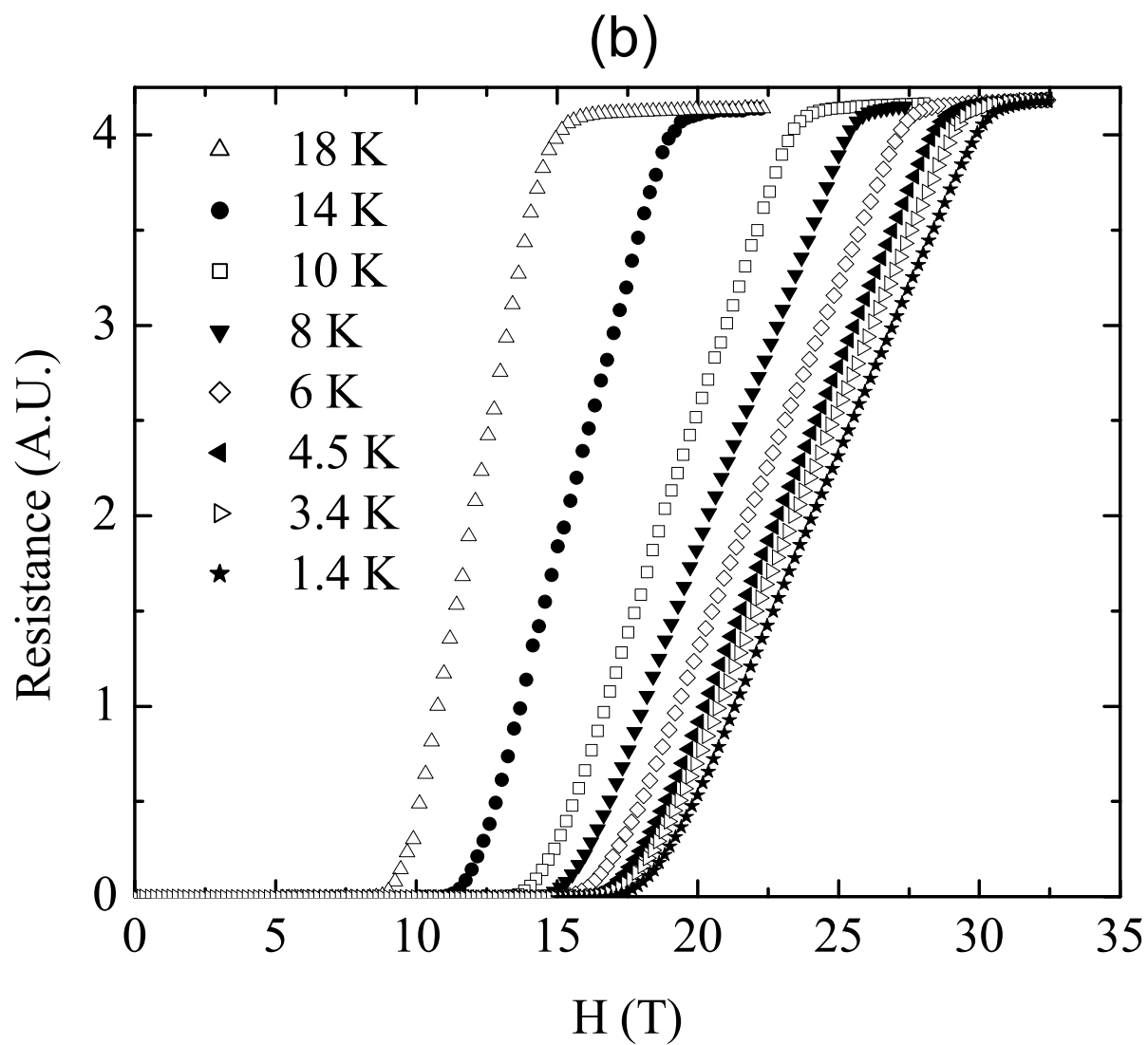


Fig. 8. Resistivity versus temperature (a) and resistivity versus field (b) for a sample annealed at 500 °C for 1000 hours.

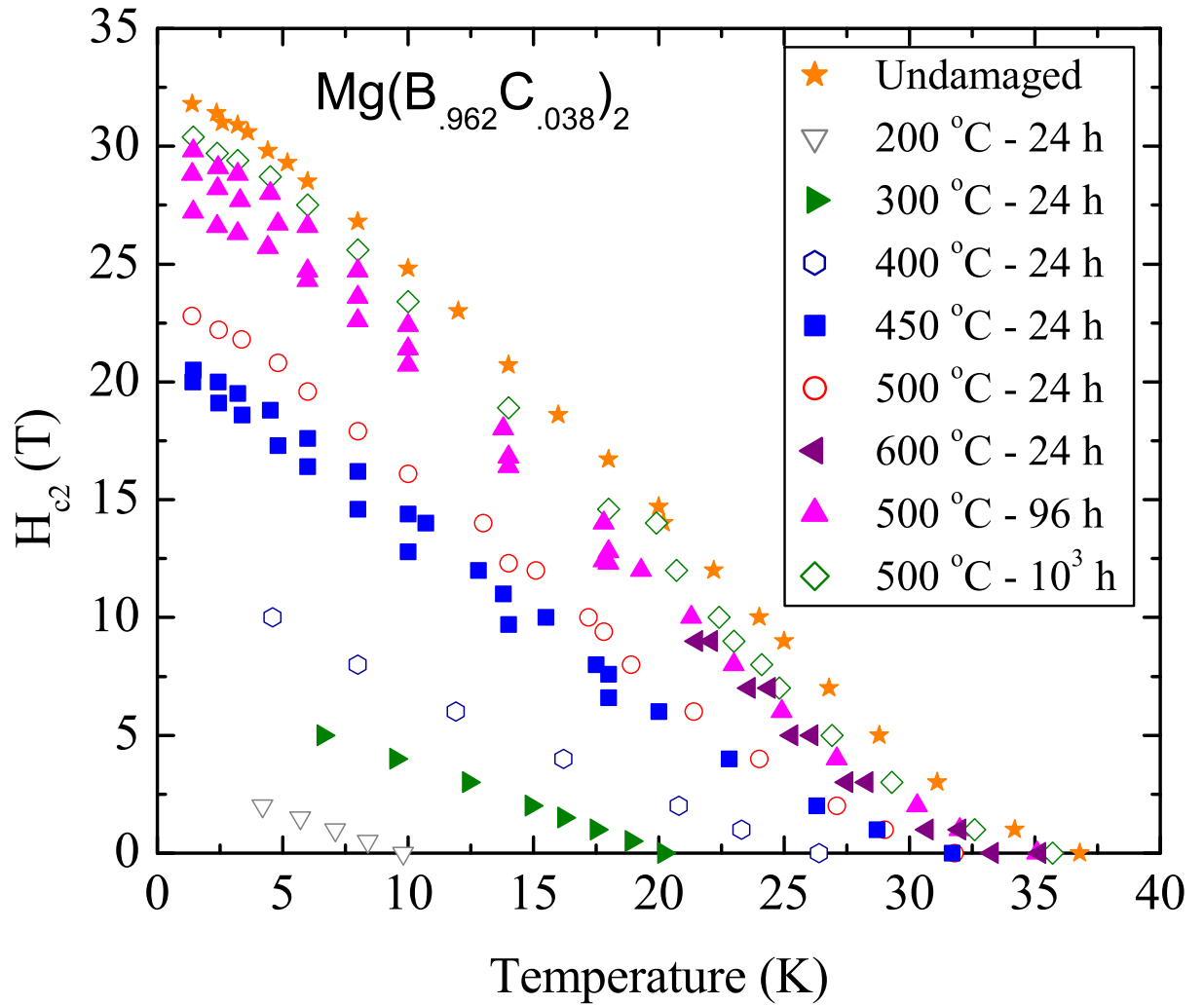
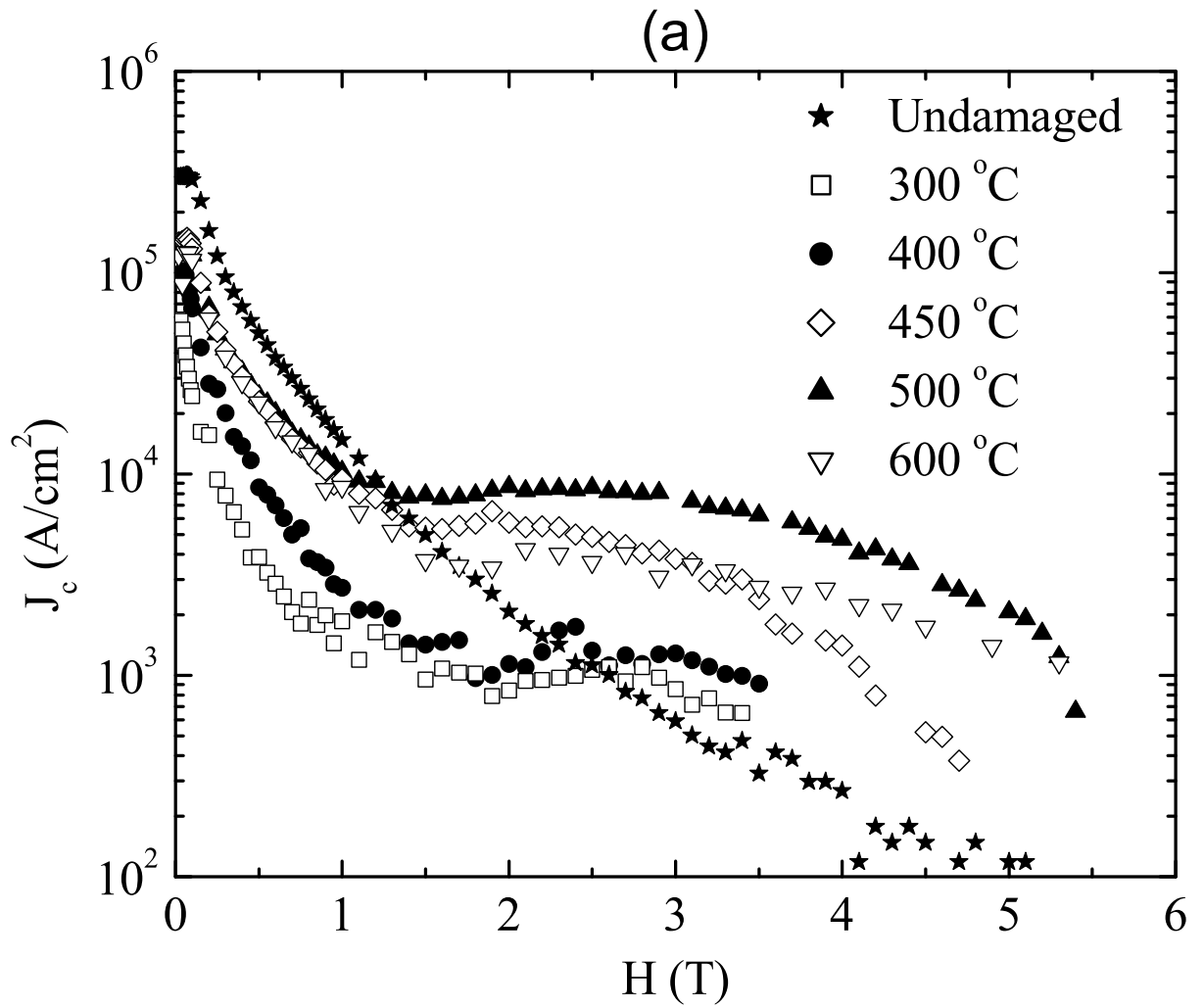


Fig. 9. Upper critical field curves for samples annealed for 24 hours at various temperatures and samples annealed for various times at 500 °C. Multiple data sets exist for the 450 °C/24 hour and 500 °C/96 hour anneals. $H_{c2}(T=0)$ approximately scales with T_c .



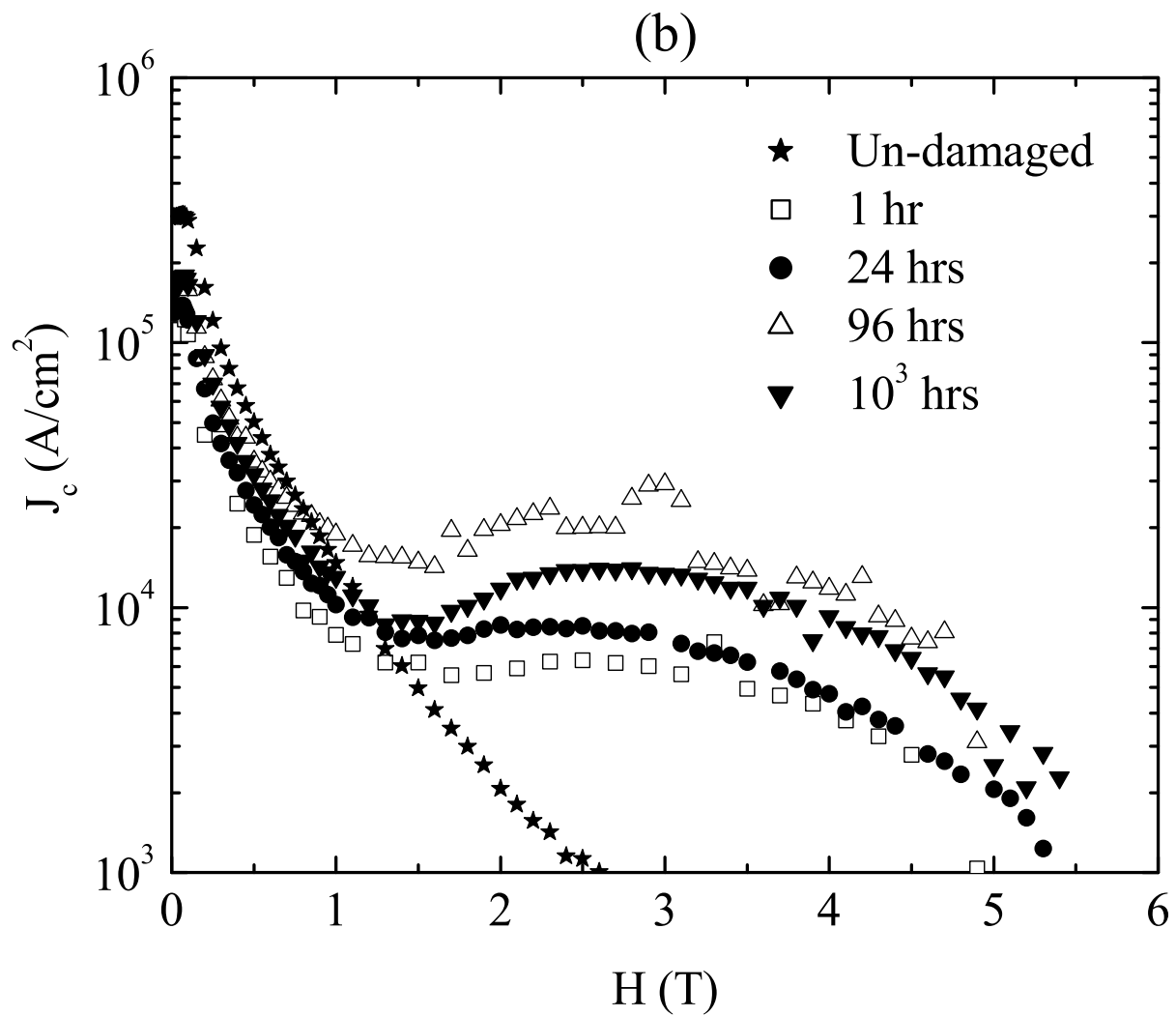


Fig. 10. Critical current densities at 5 K inferred from magnetization hysteresis loops. (a) Samples annealed at various temperatures for 24 hours. (b) Samples annealed at 500 °C for various times.

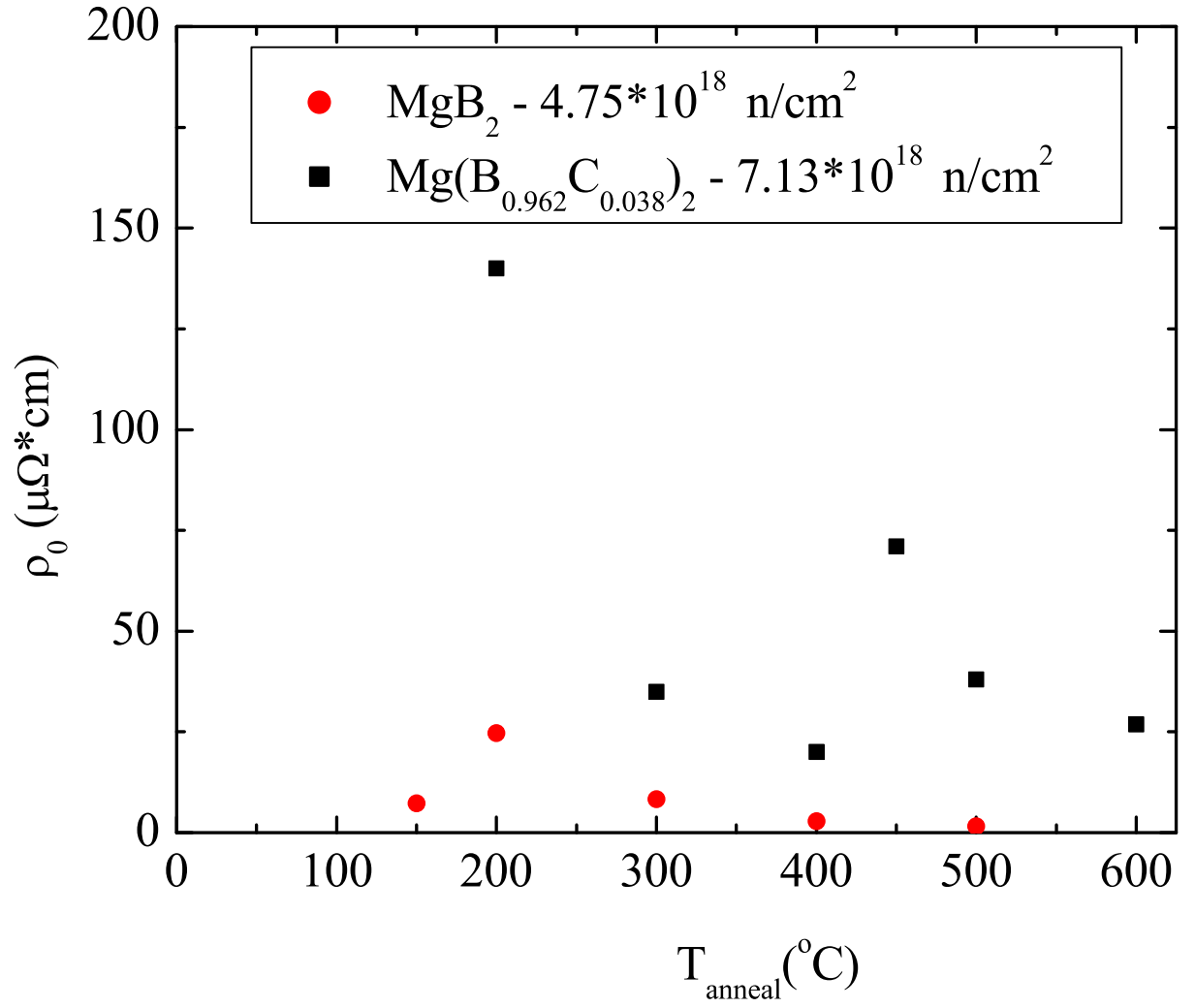


Fig. 11. Evolution of the normal state resistivity as a function of annealing temperature in neutron irradiated pure and carbon doped MgB_2 filaments.